Models for Peroxidase Compound I: Generation and Spectroscopic Characterization of New Oxoferryl Porphyrin π Cation Radical Species

D. Mandon and R. Weiss*

Institut Le Bel,[1] Université Louis Pasteur, rue Blaise Pascal, 67070 Strasbourg, France

K. Jayaraj and A. Gold*

Department of Environmental Sciences and Engineering, University of North Carolina at Chapel Hill, Chapel Hill, North Carolina 27599-7400

J. Terner*

Department of Chemistry, Virginia Commonwealth University, Richmond, Virginia 23284-2006

E. Bill and A. X. Trautwein*

Institut für Physik, Medizinische Universität zu Lübeck, 2400 Lübeck 1, FRG

Received June 4, 1992

Oxoferryl porphyrin π cation radical species have been generated by the oxidative action of *m*-chloroperoxybenzoic acid on the triflato complexes of [tetrakis(2,6-dichlorophenyl)porphyrinato]- and [tetrakis(2,4,6-trimethoxyphenyl)-porphyrinato]-iron(III) in methylene chloride/methanol-d_4. The new high-valent complexes have been characterized by a variety of spectroscopic techniques and compared to the oxoferryl porphyrin π cation radical complex generated from [tetramesitylporphyrinato]iron(III) triflate. The UV–vis and ^{1}H NMR spectra of the oxidized species are qualitatively similar. In the EPR, the complexes all show ferromagnetic coupling between ferryl and porphyrin π cation radical spins yielding quartet states. However, the average effective g values of the x,y EPR transitions, $\langle g_{x,y}^{\text{eff}} \rangle$, indicate that spin coupling is not as strong as assumed in earlier studies. A self-consistent set of parameters D, D/E, J° and $\bar{J}^{d}$ has been derived for the tetramesityl- and tetrakis(2,6-dichlorophenyl)porphyrin complexes from simulations of EPR and Mössbauer spectra; in the case of the tetrakis(2,4,6-trimethoxyphenyl)porphyrin complex, the parameters have been derived from EPR simulations alone because of difficulties in obtaining good-quality Mössbauer data. D is similar in magnitude for all three complexes, while J° exhibits magneto-structural variations. Nonzero values for $\bar{J}^{d}$ indicate a small anisotropy in the coupling of all three complexes. The resonance Raman spectra of the high-frequency region show that the marker bands ν_2, ν_{11}, and ν_4 of all three complexes behave as expected for formation of π porphyrin radicals, supporting the assignment of the oxoferryl porphyrin π cation radical structure to the oxidized species.

Introduction

Oxoferryl porphyrin π cation radical species, at two oxidation equivalents above the resting iron(III) porphyrinates, occur as intermediates in the reactions of several peroxidases and catalase with hydrogen peroxide.[2-6] An intermediate of this type has also been postulated to be the oxygen-donating species in the catalytic cycle of cytochromes P-450.[7] Despite the importance of these catalytically active species, only one model compound, the oxoferryl tetramesitylporphyrin π cation radical complex $[Fe^{IV}{=}O(TMP)]^+$, has been extensively studied to date.[8-20]

The oxoferryl porphyrin π cation radical nature of compound I of horseradish peroxidase (HRP I), in which the proximal axial

(1) Laboratoire de Cristallochimie et de Chimie Structurale (UA 424).
(2) Schulz, C. E.; Devaney, P. W.; Winkler, H.; Debrunner, P. G.; Doan, N.; Chiang, R.; Rutter, R.; Hager L. P. *FEBS Lett.* **1979**, *103*, 102–105.
(3) Roberts, J. E.; Hoffman, B. M.; Rutter, R.; Hager, L. P. *J. Biol. Chem.* **1981**, *256*, 2118–2121.
(4) Schulz, C. E.; Rutter, R.; Sage, J. T.; Debrunner, P. G.; Hager, L. P. *Biochemistry* **1984**, *23*, 4743–4754.
(5) Rutter, R.; Hager, L. P.; Dhonau, H.; Hendrich, M.; Valentine M.; Debrunner, P. G. *Biochemistry* **1984**, *23*, 6809–6816.
(6) Dolphin, D.; Felton, R. H. *Acc. Chem. Res.* **1974**, *7*, 26–32.
(7) Ortiz de Montellano, P. R. In *Cytochrome P-450: Structure, Mechanisms and Biochemistry*; Ortiz de Montellano, P. R., Ed.; Plenum Press: New York, 1986; pp 217–272.
(8) Groves, J. T.; Haushalter, R. C.; Nakamura, M.; Nemo, T. E.; Evans, B. J. *J. Am. Chem. Soc.* **1981**, *103*, 2884–2886.
(9) Groves, J. T.; Watanabe, Y. *J. Am. Chem. Soc.* **1986**, *108*, 507–508.
(10) Boso, B.; Lang, G.; McMurry, T. J.; Groves, J. T. *J. Chem. Phys.* **1983**, *79*, 1122–1126.
(11) Penner-Hahn, J. E.; McMurry, T. J.; Renner, M.; Latos-Grazinski, L.; Smith-Eble, K.; Davis, I. M.; Balch, A. L.; Groves, J. T.; Dawson, J. H.; Hodgson, K. O. *J. Biol. Chem.* **1983**, *258*, 12671–12764.
(12) Groves, J. T.; McMurray, T. J. *Rev. Port. Quim.* **1985**, *27*, 102–103.
(13) Penner-Hahn, J. E.; Eble, K. S.; McMurry, T. J.; Renner, M.; Balch, A. L.; Groves, J. T.; Dawson, J. H.; Hodgson, K. O. *J. Am. Chem. Soc.* **1986**, *108*, 7819–7825.
(14) Hashimoto, S.; Tatsuno, Y.; Kitagawa, T. *J. Am. Chem. Soc.* **1987**, *109*, 8096–8097.
(15) Groves, J. T.; Watanabe, Y. *J. Am. Chem. Soc.* **1988**, *110*, 8443–8452.
(16) Kincaid, J. R.; Schneider, A. J.; Paeng, K.-J. *J. Am. Chem. Soc.* **1989**, *111*, 735–737.
(17) Gold, A.; Jayaraj, K.; Doppelt, P.; Weiss, R.; Bill, E.; Ding, X.-Q.; Bominaar, E. L.; Trautwein, A. X.; Winkler, H. *New J. Chem.* **1989**, *13*, 169–172.
(18) Bill, E.; Ding, X.-Q.; Bominaar, E. L.; Trautwein, A. X.; Winkler, H.; Mandon, D.; Weiss, R.; Gold, A.; Jayaraj, K.; Hatfield, W. E.; Kirk, M. L. *Eur. J. Biochem.* **1990**, *188*, 665–672.
(19) Proniewicz, L. M.; Paeng, I. R.; Nakamoto, K. *J. Am. Chem. Soc.* **1991**, *113*, 3294–3303.

0020-1669/92/1331-4404$03.00/0 © 1992 American Chemical Society

ligand is either a histidine–imidazole[5] or –imidazolate,[21] and chloroperoxidase compound I (CPO-I), in which the proximal axial ligand is a cysteinate,[22] has been established for a number of years. More recently, the oxoferryl π cation radical electronic structure has also been firmly established for the model complex $[Fe^{IV}{=}O(TMP)]^+$, where the second axial ligand of iron may be either methanol[12,20] or *m*-chlorobenzoate.[15,20] Despite general similarities in the physicochemical descriptors of enzymic and model species, some important parameters of electronic structure differ significantly. In particular, the magnetic coupling J between the porphyrin π cation radical and the iron(IV)–oxo unit, which was shown to be weakly ferromagnetic in HRP-I[2,3] and stronger but antiferromagnetic in CPO-I,[5] is strong and clearly ferromagnetic[10] in the model derivative $[Fe^{IV}{=}O(TMP)]^+$. The initial report on the Mössbauer spectroscopy of $[Fe^{IV}{=}O(TMP)]^+$ did not take coupling into account directly, but approximated the system using an $S = {}^3/_2$ ground state.[10] The first estimates of J were derived from a spin Hamiltonian analysis of magnetic Mössbauer spectra,[17,18] which yielded only an approximation because of the necessity of restricting the number of spin Hamiltonian parameters in the absence of complementary spectroscopic methods.

In order to obtain a better understanding of the electronic structure of the iron(IV)–oxo tetraarylporphyrin π radical cation complexes, we have generated and spectroscopically characterized additional examples of oxoferryl π cation radical complexes from the following porphyrins: tetrakis(2,6-dichlorophenyl)porphyrin (TDCPP),[23] tetrakis(2,4,6-trimethoxyphenyl)porphyrin (TTMPP),[24] and "picket-fence" porphyrin ($TP_{piv}P$).[25] In this paper, we report the EPR and Mössbauer spectra of $[Fe^{IV}{=}O(TDCPP)]^+$ and the EPR spectrum of $[Fe^{IV}{=}O(TTMPP)]^+$. For comparison, we have also included data on $[Fe^{IV}{=}O(TMP)]^+$ and use complementary analysis of EPR and Mössbauer spectra to improve the description of coupling in the model complexes. The resonance Raman spectra in the high-frequency region, as well as the UV–vis and ^1H NMR spectra of $[Fe^{IV}{=}O(TDCPP)]^+$ and $[Fe^{IV}{=}O(TTMPP)]^+$ are given and compared to data from $[Fe^{IV}{=}O(TMP)]^+$.

Experimental Section

Instrumentation. UV–vis spectra were recorded on a Cary 219 spectrophotometer equipped with a variable-temperature Dewar using a quartz cuvette with a 0.1-cm path length. ^1H NMR spectra were recorded on a Bruker WP 200 spectrometer at 200 MHz.

EPR spectra were recorded on a Bruker ER200 D-SRC spectrometer equipped with an Oxford Instruments liquid-helium cryostat, Model ESR 910, which permits regulation of sample temperature down to 2.7 K. Temperature measurements were calibrated using Curie-Weiss behavior of the signal of a ferric low-spin standard (ferric cytochrome *c*).[26] Temperature stability was on the order of 0.2 K, and from measurements with a carbon glass resistor, the temperature gradient across the sample was found to be less than 0.5 K. For spin quantitation, EPR spectra were numerically doubly integrated and weighted by a factor to account for the influence of anisotropic effective g values on the transition probabilities.[27] Integrations were performed at 4.2 K, and the effects of zero-field splittings were neglected. In order to avoid passage effects, the field-modulation frequency was reduced to 1.6 kHz for spin quantitations as well as for measurements of temperature dependences.

The Mössbauer spectrometer worked in the conventional constant acceleration mode with a source of 1.85 GBq $^{57}Co/Rh$ (Amersham Buchler). From calibration measurements, the standard line width was 0.23 mm s^{-1}. Isomer shifts are given relative to metallic iron (α-Fe) at room temperature. The Mössbauer cryostats were helium-bath cryostats (MD 306, Oxford Instruments). The γ-beam could be transmitted parallel or perpendicular to the applied field. The sample temperature in the cryomagnet was regulated with a variable-temperature insert. A small field of 20 mT could be applied to the tail of the bath cryostat with a permanent magnet.

Resonance Raman signals were detected by an optical multichannel analyzer (EG&G Princeton Applied Research Corp., Model 1215/1216) with a cooled (–50 °C) Model 1254 silicon intensified vidicon detector head that was coupled to a 0.5-m spectrograph (Spex Model 1870) containing an 1800 groove/mm holographic grating (Jobin–Yvon/Instruments SA). The excitation source was a krypton ion laser (Spectra-Physics Model 171) equipped with an ultra-high-field magnet. The sample was contained in a spinning quartz cell (Spex) that was maintained at –80 °C in a thermostated plastic enclosure with cold N_2 gas. Scattered light was collected at 90° through an optically clear wall of the enclosure by a 50-mm $f/0.95$ Canon lens and imaged by a quartz 180-mm $f/4.5$ lens (Melles Griot).

Spin-Hamiltonian Analysis. For the analysis of both magnetic Mössbauer spectra and EPR spectra of the coupled iron(IV) ($S = 1$) porphyrin radical ($S' = {}^1/_2$ system, we adopted the spin Hamiltonian including spin coupling

$$H_e = D[S_z^2 - {}^2/_3 + E/D(S_x^2 - S_y^2)] + \beta\left(\vec{S}\cdot\overline{\overline{g}} + g'\vec{S}'\right)\cdot\vec{B} - \vec{S}\cdot\overline{\overline{J}}\cdot\vec{S}' \quad (1)$$

with the parameters having their usual meanings. The coupling tensor $\bar{J}$ was divided into an isotropic part $\bar{J}^o$ and a traceless anisotropic contribution $\bar{J}^d$. The g tensor of the ferryl iron was related to the zero-field splitting using the perturbation formula derived from a ligand-field treatment by Oosterhuis and Lang[28] (with the one-electron spin–orbit coupling constant taken as $\zeta = 500$ cm^{-1}). For the radical spin, g' was fixed at 2.

The inhomogeneous EPR spectra were simulated with eq 1 using a "g-strain" model for the line shape,[4] which is based on a Gaussian distribution of spin-Hamiltonian parameters and which leads to an angular variation of Gaussian line widths of spin packets. The relevant parameters which were distributed are the rhombicity E/D and the isotropic spin-coupling constant J^o. The values $\sigma(x)$ given in Table III represent the widths of the Gaussian distributions $(2\pi\sigma^2)^{-1/2}\exp(-x^2/2\sigma^2)$ of these parameters. Mössbauer spectra were simulated using eq 1 together with the usual nuclear Hamiltonian.[2]

Reagents. Methylene chloride was distilled from calcium hydride prior to use. Reagent grade *m*-chloroperoxybenzoic acid (mCPBA) was obtained by evaporation of a dried (Na_2SO_4) solution of commercial material (Aldrich Chemical Co.). [Tetramesitylporphyrinato]iron(III) chloride ([Fe^{III}(Cl)TMP]), [tetramesitylporphyrinato]iron(III) triflate ([Fe^{III}(Tf)TMP]), [tetrakis(2,6-dichlorophenyl)porphyrinato]iron(III) triflate ([Fe^{III}(Tf)TDCPP]), [tetrakis(2,4,6-trimethoxyphenyl)porphyrinato]iron(III)triflate ([Fe^{III}(Tf)TTMPP]), and the ^{57}Fe-enriched complexes were prepared and purified by published methods,[29–32] and all spectroscopic data were consistent with assigned structures.

Sample Preparation. Oxidations of the iron(III) porphyrins were performed in toluene/methanol-d_4 (6:1) and methylene chloride/methanol-d_4 (6:1) for the TMP complexes and in methylene chloride/methanol-d_4 (6:1) for the TDCPP and TTMPP derivatives at –80 °C by addition of an approximately 4-fold molar excess of mCPBA in methanol-d_4 to a solution of the porphyrin ($\approx 10^{-3}$ M) in toluene or methylene chloride. Techniques for obtaining UV–vis, ^1H NMR and EPR samples have been described in detail elsewhere.[17,18] Samples for resonance Raman spectroscopy were generated by addition of mCPBA in methanol-d_4 to a cooled methylene chloride solution of the porphyrin in the spinning cell. The laser wavelength used was 406.7 nm. The resonance Raman spectra were calibrated with the known frequencies of indene, cyclohexene, and fenchone. The resolution was 1 cm^{-1}, and band frequencies are accurate

(20) Hashimoto, S.; Mizutani, Y.; Tatsuno, Y.; Kitagawa, T. *J. Am. Chem. Soc.* **1991**, *113*, 6542–6549.
(21) Roberts, J. E.; Hoffman, B. M.; Rutter, R.; Hager, L. P. *J. Am. Chem. Soc.* **1981**, *103*, 7654–7656.
(22) Dawson, J. H.; Kaw, L.-S.; Penner-Hahn, J. E.; Sono, M.; Eble, K. S.; Bruce, G. S.; Hager, L. P.; Hodgson, K. O. *J. Am. Chem. Soc.* **1986**, *108*, 8114–8116.
(23) Traylor, P. S.; Dolphin, D.; Traylor, T. G. *J. Chem. Soc., Chem. Commun.* **1984**, 279–280.
(24) Vaska, L.; Amundsen, A. R.; Brady, R.; Flynn, B. R.; Nakai, H. *Finn. Chem. Lett.* **1974**, 66–69.
(25) Collman, J. P.; Gagne, R. R.; Halbert, T. R.; Marchon, J.-C.; Reed, C. A. *J. Am. Chem. Soc.* **1973**, *95*, 7868–7880.
(26) Slappendel, S.; Veldink, G. A.; Vliegenhardt, J. F. G.; Aasa, R.; Malmström, B. *Biochem. Biophys. Acta* **1980**, *642*, 30–39.
(27) Aasa, R.; Vänngardm, T. *J. Magn. Reson.* **1975**, *19*, 308–315.
(28) Oosterhuis, W. T.; Lang, G. *J. Chem. Phys.* **1973**, *58*, 4757–4765.
(29) Adler, A. D.; Longo, F. R.; Kampas, F.; Kim. J. *J. Inorg. Nucl. Chem.* **1970**, *32*, 2443–2445.
(30) Reed, C. A.; Mashiko, T.; Bentley, S. P.; Kastner, M. E.; Scheidt, W. R.; Spartalian, K.; Lang, G. *J. Am. Chem. Soc.* **1979**, *101*, 2948–2958.
(31) Hill, C. L.; Williamson, M. M. *J. Chem. Soc., Chem. Commun.* **1985**, 1228–1229.
(32) Hoffmann, P.; Labat, G.; Robert, A.; Meunier, B. *Tetrahedron Lett.* **1990**, *31*, 1991–1994.

Scheme I

R=Cl, R'=H : |Fe^{III}(Tf)TDCPP|

R=R'=CH_3O : |Fe^{III}(Tf)TTMPP|

R=R'=CH_3 : |Fe^{III}(Tf)TMP|

Tf = $CF_3SO_3^-$

R=Cl, R'=H : |Fe^{IV}=OTDCPP|$^+$

R=R'=CH_3O : |Fe^{IV}=OTTMPP|$^+$

R=R'=CH_3 : |Fe^{IV}=OTMP|$^+$

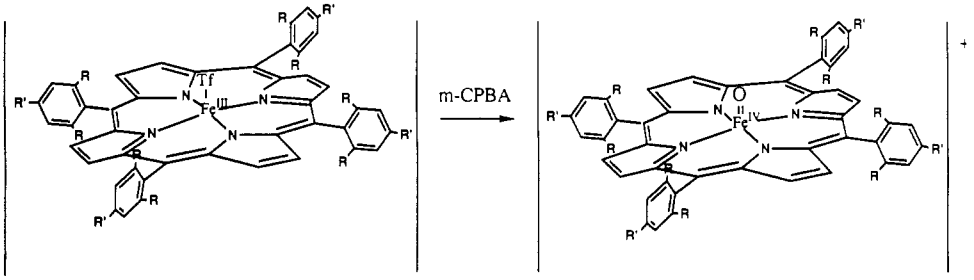

to 1 cm^{-1} for strong, isolated bands. The Mössbauer samples were generated in a delrin cup sealed with epoxy to a glass tube forming a reaction vessel that could be conveniently immersed in a cold bath. mCPBA in methanol-d_4 was added to the cooled delrin cup containing the porphyrin in methylene chloride, and the reaction was mixed by bubbling argon through until appearance of a green solution indicated formation of a oxoferryl porphyrin π cation radical. Toluene/methanol-d_4 solutions containing the oxidized TMP complex were prepared for storage or use by plunging the reactor into liquid nitrogen and removing the delrin cup from the tube with a razor knife. Reaction vessels containing [Fe^{IV}=O(TDCPP)]$^+$ or [Fe^{IV}=O(TTMPP)]$^+$ were transferred to a precooled vacuum trap and evacuated at −80 °C by a diffusion pump. Removal of methylene chloride was followed by single ion monitoring at m/z = 84 on a quadrupole mass spectrometer. When the ion current had decreased to one-tenth of its initial value (final pressure ≈ 1 × 10^{-7} Torr), the trap was removed from the vacuum line, the reaction immersed in liquid nitrogen, and the delrin cup detached from the glass tube with a razor knife for storage in liquid nitrogen or mounting in the Mössbauer sample holder.

Results and Discussion

Oxidation Reactions. mCPBA was chosen as the monooxygen donor in order to work in a homogeneous system with an oxidant of known structure. Oxidation of chloro-, hydroxo-, and (triflato)-iron(III) porphyrins has shown that with the weakly coordinated triflate counterion, a cleaner oxoferryl π cation radical of TDCPP and TTMPP can be generated (Scheme I).[17,18] Accordingly, the triflato derivatives [Fe^{III}(Tf)TDCPP] and [Fe^{III}(Tf)TTMPP] were selected as starting materials. As with TMP,[12,15] the presence of a small amount of methanol in the reaction solvent facilitates a clean oxidation. These observations presumably reflect facilitation of an initial step in the generation of the [Fe^{IV}=O]$^+$ species involving coordination of mCPBA to the iron(III) center. Methanol-d_4 was used in an effort to increase the lifetimes of the high-valent porphyrins by slowing reduction via abstraction of the acidic hydroxy hydrogen.[33]

All of the spectroscopic data described below unequivocally support the quantitative generation of the oxoferryl porphyrin π cation radicals [Fe^{IV}=O(TMP)]$^+$ in toluene/methanol-d_4 or methylene chloride/methanol-d_4 and [Fe^{IV}=O(TDCPP)]$^+$ and [Fe^{IV}=O(TTMPP)]$^+$ in methylene chloride/methanol-d_4.

Electronic Spectra. Oxidation of the triflates by mCPBA is accompanied by formation of deep green solutions typical of those reported for the oxidation of ferric TMP derivatives.[8,9,15] The UV–vis spectral parameters of the oxidized complexes in methylene chloride/methanol-d_4 are given in Table I. They are qualitatively similar to those of [Fe^{IV}=O(TMP)]$^+$, having a low-intensity Soret absorbance at 400 nm and a second band at ≈670 nm.

Table I. UV–vis Spectra at −80 °C in CH_2Cl_2/CD_3OD (6:1)

complex	λ_{max} (nm) ($\epsilon \times 10^{-3}$)	ref
[Fe^{IV}=O(TDCPP)]$^+$	391 (79.9), 678 (10.7)	*a*
[Fe^{IV}=O(TTMPP)]$^+$	394 (42.6), 670 (3.71)	*a*
[Fe^{IV}=O(TMP)]$^+$	406 (61.3), 674 (7.6)	9,*b*

a This work. *b* Molar extinction coefficients and λ_{max} estimated from UV–vis trace in ref 9, assuming a 1-cm path length.

Table II. ^{1}H NMR Spectra of Oxoferryl Porphyrin Cation Radicals

compound	freq (MHz)	solvent	temp (°C)	proton shifts (ppm) *m*-H	proton shifts (ppm) py-H	ref
[Fe^{IV}=O(TDCPP)]$^+$	200	CD_2Cl_2/CD_3OD	−60	31	−60.8	*a*
[Fe^{IV}=O(TTMPP)]$^+$	200	CD_2Cl_2/CD_3OD	−70	31.6, 36.0	−33.2	*a*
[Fe^{IV}=O(TMP)]$^+$	360	CD_2Cl_2/CD_3OD	−77	68	−27	8

a This work.

^{1}H NMR Spectra. The ^{1}H NMR shifts of the phenyl meta and pyrrole β proton resonances of [Fe^{IV}=O(TDCPP)]$^+$ and [Fe^{IV}=O(TTMPP)]$^+$ are identified in Table II. The pattern of shifts is similar to that of the corresponding protons[8,34] of [Fe^{IV}=O(TMP)]$^+$, which are included in Table II for reference. Although the pyrrole protons of all oxoferryl porphyrin cation radicals appear upfield of TMS and the phenyl meta protons of all complexes appear downfield, the magnitude of the shifts varies dramatically. However, the separation between the meta and pyrrole signals of each complex, $\Delta\delta$(pyrrole − meta) correlates directly with the effective g values for the x,y EPR transitions (given below), with a similar $\Delta\delta$ for TMP (95 ppm) and TDCPP (92 ppm) and a smaller $\Delta\delta$ for TTMPP (67 ppm).

EPR and Mössbauer Spectra. The X-band EPR spectra of [Fe^{IV}=O(TDCPP)]$^+$, [Fe^{IV}=O(TTMPP)]$^+$, and [Fe^{IV}=O(TMP)]$^+$ were recorded in the temperature range 2.7–30 K. Absorption-derivative spectra, recorded under non-saturating conditions are shown in Figure 1a–c. Resonances at approximately g^{eff} = 4 and 2 are typical of spin-quartet species[35] and confirm that ferryl iron (S = 1) is ferromagnetically coupled to the porphyrin radical (S' = $^1/_2$). The EPR signals originate from the $|S_t = {}^3/_2, M_t = \pm{}^1/_2\rangle$ Kramers doublet, which is energetically separated from the EPR-silent excited-state $|S_t = {}^3/_2, M_t = \pm{}^3/_2\rangle$ Kramers doublet. Spin quantitations of the three complexes and comparison with the high-spin ferric signals of the starting solutions show virtually quantitative conversion of the TDCPP and TMP complexes to the oxidized quartet species

(33) Gold, A.; Jayaraj, K.; Doppelt, P.; Weiss, R.; Chottard, G.; Bill, E.; Ding, X.-Q.; Trautwein, A. X. *J. Am. Chem. Soc.* **1988**, *110*, 5756–5761.

(34) Balch, A. L.; Latos-Grazynski, L.; Renner, M. W. *J. Am. Chem. Soc.* **1985**, *107*, 2983–2985.

(35) Weltner, W. *Magnetic Atoms and Molecules*; Dover: New York, 1983, pp 236–256.

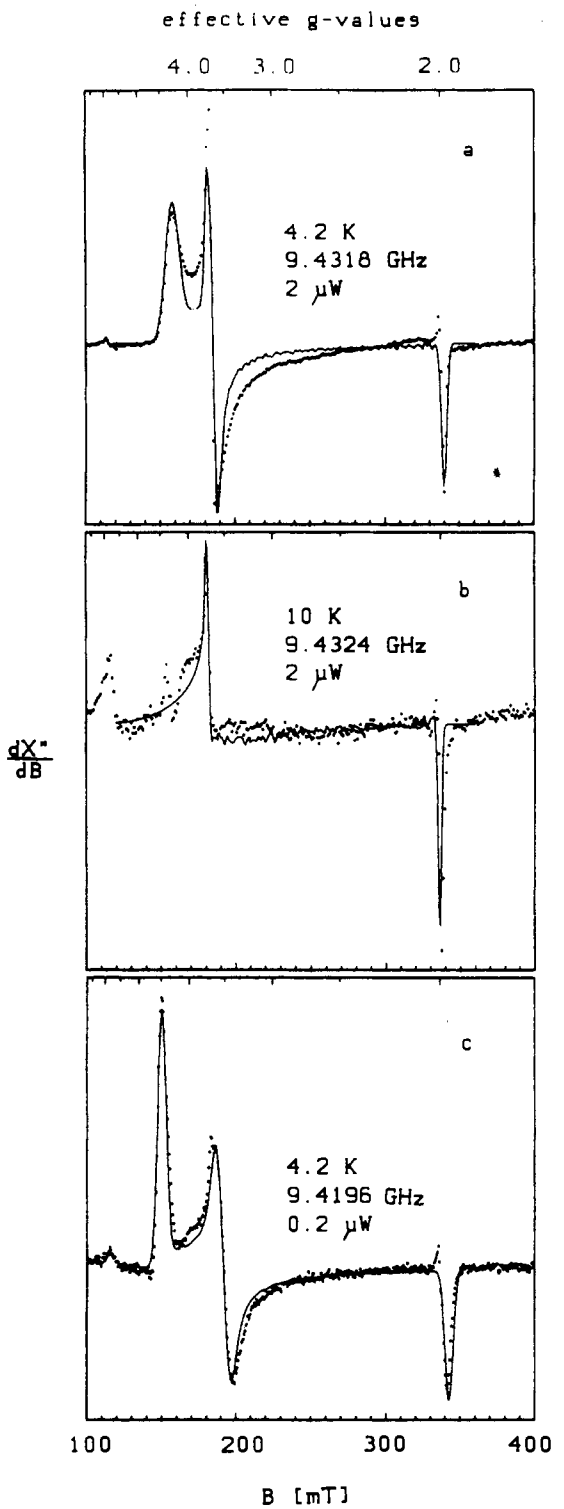

Figure 1. EPR spectra of $[Fe^{IV}{=}O(TDCPP)]^+$ (a), $[Fe^{IV}{=}O(TTMPP)]^+$ (b), and $[Fe^{IV}{=}O(TMP)]^+$ (c). The solid lines are simulations based on the spin Hamiltonian (eq 1) and the line-shape model described in the text. The spectra are calculated using the parameters given in Table III. The spin-Hamiltonian parameters are consistent with effective g values of g_x^{eff}, g_y^{eff}, and g_z^{eff} of 4.26, 3.62, and 1.98 for a, 3.71, 3.71, and 1.99 for b, and 4.47, 3.50, 1.98 for c.

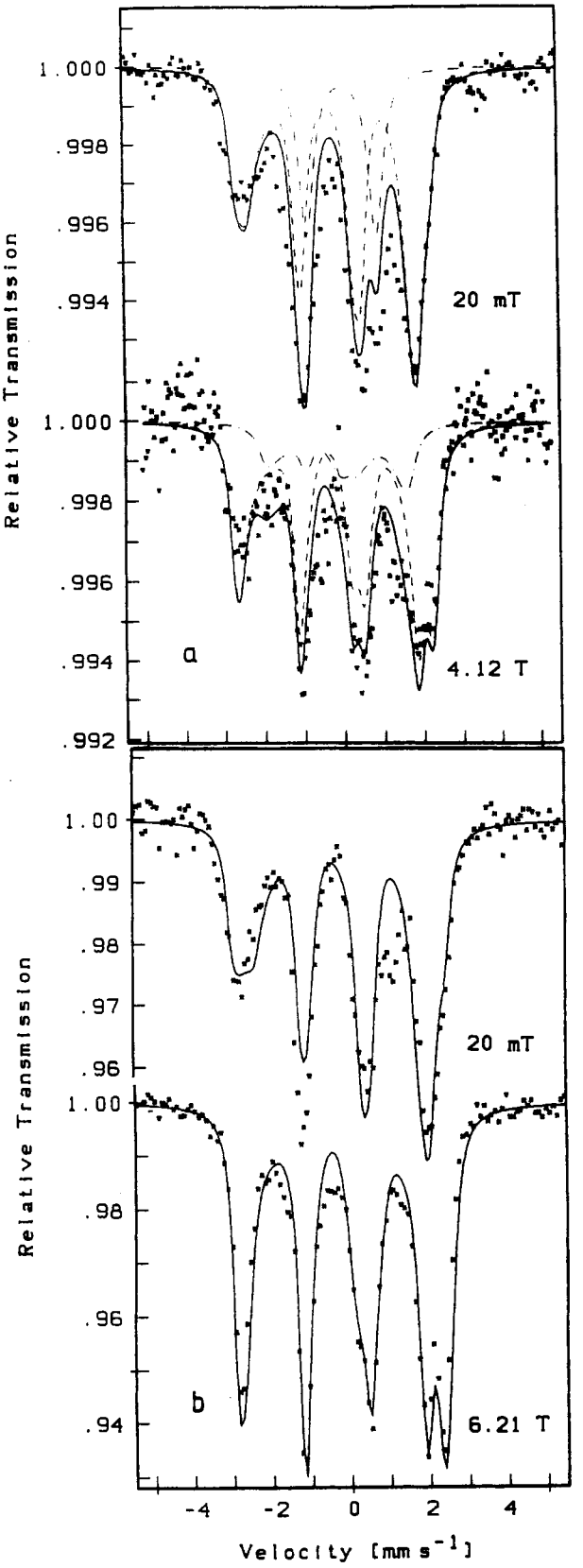

Figure 2. Mössbauer spectra of a vacuum-dried sample of $[Fe^{IV}{=}O(TDCPP)]^+$ (a) and of $[Fe^{IV}{=}O(TMP)]^+$ (b) recorded at 4.2 K in fields of 20 mT, 4.21 T, and 6.21 T applied perpendicular to the γ-rays. The dashed lines are spin-Hamiltonian simulations calculated in slow relaxation limit using the parameters given in Table III. The dashed–dotted lines in part a represent an oxoferryl contamination of 24%. These subspectra are simulated using eq 1 without coupling term and parameters. $D = 25$ cm^{-1}, $E/D = 0.075$, $g = (2.2, 2.24, 1.99)$, $\Delta E_Q = 1.48$ mm s^{-1}, $\eta = 0$, $A/g_N\beta_N = (-24.5, -24.5, -6)$ T, $\delta = 0.06$ mm s^{-1}.

and 90% conversion of the TTMPP complex. Similar high conversions were achieved for samples prepared for Mössbauer spectroscopy (Figure 2). Since the starting complex $[Fe^{III}(Tf)$-TDCPP] is not soluble in toluene, Mössbauer samples of $[Fe^{IV}{=}O(TDCPP)]^+$ were generated in methylene chloride/methanol-d_4, and because of the high mass absorption of γ-rays by chlorine, methylene chloride was removed by vacuum drying. This procedure resulted in contamination with 24% of an oxoferryl impurity, as revealed by the spectral simulations. The occurrence of a reduced impurity during the 0.5 h required for vacuum drying is not surprising in view of previous observations of the facile

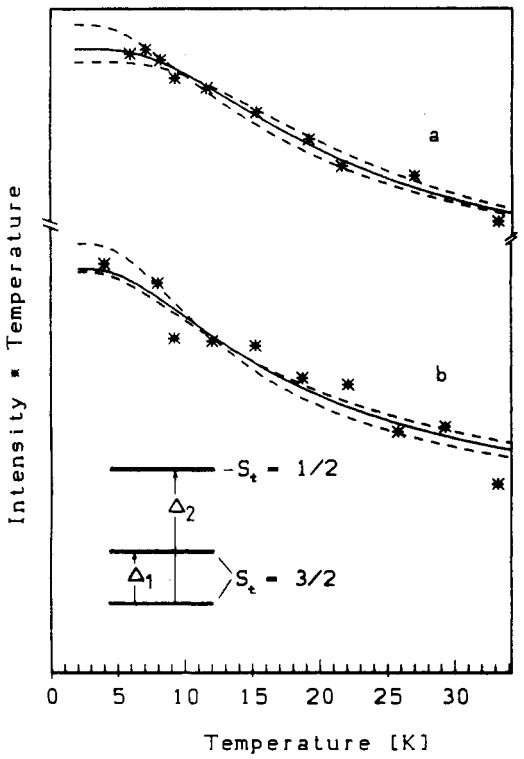

Figure 3. Temperature dependence of EPR intensities of $[Fe^{IV}{=}O(TDCPP)]^+$ (a) and $[Fe^{IV}{=}O(TTMPP)]^+$ (b). The experimental data are obtained by double integration of spectra recorded under nonsaturating conditions with a 1.6-KHz modulation frequency in order to avoid passage effects. The solid lines are fits of the thermal population of the ground doublet $p(T) = [1 + \exp(-\Delta_1/KT) + \exp(-\Delta_2/KT)]^{-1}$, yielding values for Δ_1 and Δ_2 of 22 and 38 cm^{-1}, respectively for part a and 15 and 31 cm^{-1}, respectively, for part b. The dashed line represent regions of error in Δ_1 of ± 3 cm^{-1}; similar curves are found for variations in Δ_2 of ± 8 cm^{-1}. A corresponding analysis for $[Fe^{IV}{=}O(TMP)]^+$ (not shown) gave values of $\Delta_1 = 24$ cm^{-1} and $\Delta_2 = 45$ cm^{-1}.

reduction of the oxoferryl porphyrin π cation radical system.[33] $[Fe^{III}(Tf)TTMPP]$ posed similar solubility problems; however, all attempts to vacuum dry methylene chloride/methanol solutions of $[Fe^{IV}{=}O(TTMPP)]^+$ resulted in complete reduction of the sample. For $[Fe^{IV}{=}O(TMP)]^+$ and $[Fe^{IV}{=}O(TDCPP)]^+$, the 4.2 K Mössbauer spectra support the EPR findings. The magnetic hyperfine splitting due to internal fields of $\approx$13 T reveals spin-expectation values of $\langle S \rangle \approx 1$, which is in accord with a $|S_t = {}^3/_2, M_t = \pm{}^1/_2\rangle$ ground state, as reported in previous Mössbauer studies.[17,18]

The splittings Δ_1 and Δ_2 between the two Kramers doublets in the $S_t = {}^3/_2$ manifold and between the $S_t = {}^3/_2$ and $S_t = {}^1/_2$ manifolds were evaluated from the temperature dependences of the EPR intensities (Figure 3). The values of Δ_1 indicate large zero-field splittings of ferryl iron ($D \geq 20$ cm^{-1}), which in the ligand-field model[5,28] leads to local $g_{x,y}$ values for iron of about 2.2. With these values, x,y-transitions would be expected at an average effective g factor of about 4.3 in a system of "infinitely" strong coupling with spin manifolds completely isolated energetically. The discrepancy between the predicted value of 4.3 and observed values of less than 4 (Figure 1) therefore shows that exchange coupling in the complexes is not "infinitely" strong, but of the same order of magnitude as D. The competition of zero-field and exchange interaction leads to mixing of spin states and to a dependency of effective g factors on $|J^\circ|$ and D.[5] In this situation, a proper description of the system requires diagonalization of the full spin-Hamiltonian (eq 1). For $[Fe^{IV}{=}O(TMP)]^+$ and $[Fe^{IV}{=}O(TDCPP)]^+$, a unique set of electronic parameters was determined from simulations of EPR and Mössbauer spectra using the constraints that D, E, and J° must

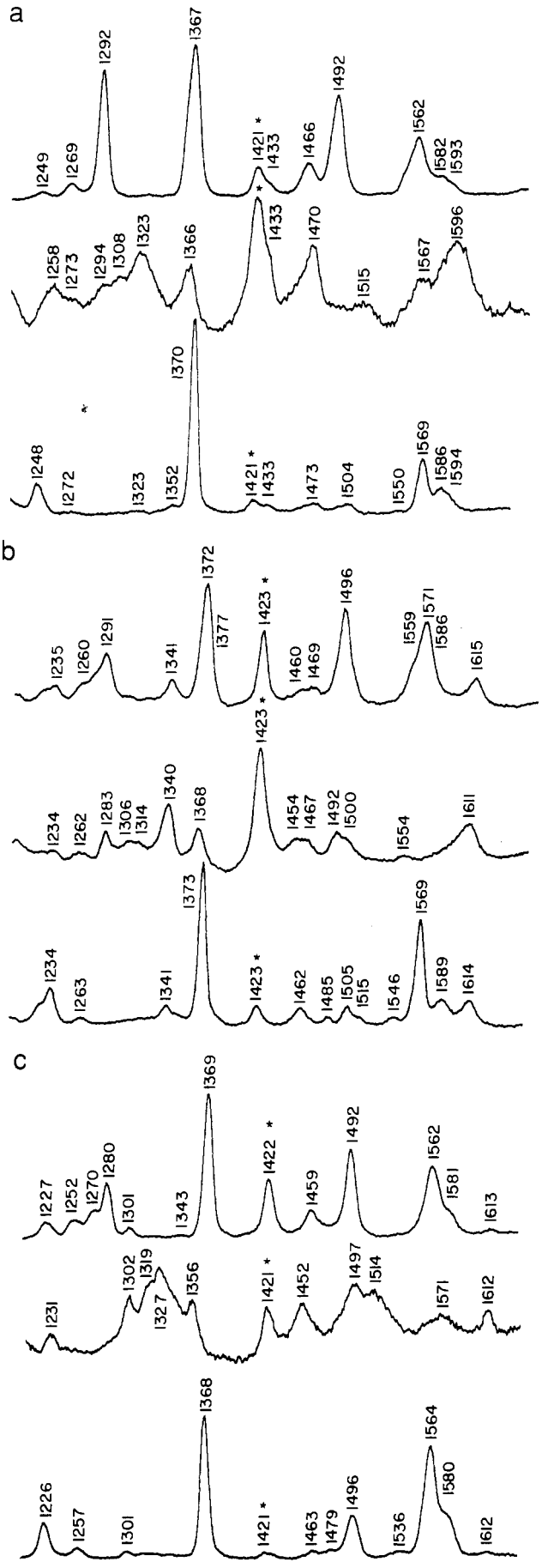

Figure 4. Resonance Raman spectra of (a) TDCPP, (b) TTMPP, and (c) TMP complexes in methylene chloride/methanol-d_4 at -80 °C with excitation at 406.7 nm. Key: top trace, ferric complex; middle trace, oxidized complex; bottom trace, ferric species after addition of excess imidazole.

Table III. Spin-Hamiltonian and Mössbauer Parameters of Oxoferryl Porphyrin Cation Radical Complexes[a]

compound	D (cm^{-1})	E/D	$\bar{g}$ [b]	ΔE_Q (mm s^{-1})	η	$\delta_{\alpha\text{-Fe}}$ (mm s^{-1})	$A_x = A_y$ (T)	A_z (T)	J° (cm^{-1})	$\bar{J}$ [d] (cm^{-1})
[Fe^{IV}=O(TDCPP)]$^+$	25	0.07	2.20, 2.24, 1.99	1.48	0	0.06	−24.5	−6.0	+38[c]	+1.6, −3.2, +1.6
[Fe^{IV}=O(TTMPP)]$^+$	20	0[d]	2.17, 2.17, 1.99						+22	−1.5, −1.5, +3.0
[Fe^{IV}=O(TMP)]$^+$	25	0.04[e]	2.21, 2.23, 1.99	1.62	0	0.08	−25.0	−5.0	+43	+1.7, −3.4, +1.7

[a] The electronic Hamiltonian is given by eq (1). The components of the A tensor are part of the usual nuclear Hamiltonian. The values of quadrupole splitting ΔE_Q, asymmetry η and isomer shift δ correspond to 4.2 K, δ is measured relative to α-Fe at room temperature. [b] Electronic g values of ferryl iron are related to D and E/D via a ligand field model.[28] [c] Gaussian distribution of J° with $\sigma(J^\circ) = 0.8$ mT. [d] Gaussian distribution of E/D with $\sigma(E/D) = 0.14$. [e] Gaussian distribution of E/D with $\sigma(E/D) = 0.014$. The Mössbauer parameters for [Fe^{IV}=O(TDCPP)]$^+$ are from spectra of a vacuum-dried sample; for [Fe^{IV}=O(TTMPP)]$^+$ no Mössbauer spectra could be obtained.

be compatible with the observed values Δ_1 and Δ_2. For [*Fe*^{IV}=O(TTMPP)]$^+$ only EPR data were used since Mössbauer data could not be obtained (Table III).

The inhomogeneous EPR spectra were simulated using a lineshape model based on parameter distributions as described above, because initial simulations without these distributions were unsatisfactory. For [Fe^{IV}=O(TTMPP)]$^+$, the effect of a broad parameter distribution is directly visible because the EPR spectrum (Figure 1b) corresponds to the first derivative of a nearly rectangular absorption pattern. Simulations of the overall EPR features provide sensitive estimates for D and J°; however, they are strongly correlated. This becomes plausible from a perturbation treatment, which shows that to the first order, effective g values depend sensitively on the ratio $|J^\circ|/D$ and on the g values of iron.[2,18] The EPR simulations also turned out to be sensitive to the anisotropy of the J tensor. This demonstrates that in the spin-coupled systems under study here, with competing zero-field and exchange interactions, the spin states are affected even by weak perturbations.

Also, the simulations of the Mössbauer spectra are sensitively influenced by the anisotropy of $\bar{J}$. This sensitivity facilitates the optimization of parameter sets for [Fe^{IV}=O(TDCPP)]$^+$ and [Fe^{IV}=O(TMP)]$^+$, with which EPR as well as Mössbauer features could be consistently simulated. For [Fe^{IV}=O(TDCPP)]$^+$ and [Fe^{IV}=O(TMP)]$^+$, we found the ratio $|J^\circ|/D \leq 2$, with $J^\circ \approx 40$ cm^{-1} and with anisotropy contributions $\bar{J}^d \approx (-1.6, +3.2, -1.6)$ cm^{-1}. This result shows that the iron(IV)–radical spin coupling in [Fe^{IV}=O(TMP)]$^+$ is weaker than had been reported on the basis of the analysis of the Mössbauer spectral properties alone.[17,18] For [Fe^{IV}=O(TTMPP)]$^+$, which could not be investigated by Mössbauer spectroscopy, the results may be less definitive in the sense that the magnitude of the zero-field parameter D was derived from EPR studies alone. Nevertheless, the fact that the iron(IV)–radical spin coupling is weakest in this complex ($|J^\circ|/D \approx 1$, with $J^\circ \approx 25$ cm^{-1}) is obvious from the $\langle g_{x,y}^{eff} \rangle$ value, which is significantly lower than those for the other two complexes.

The EPR signals of all three oxidized complexes exhibit a rhombic splitting, $\Delta g^{eff} = |g_x^{eff} - g_y^{eff}|$, of the x,y transitions ordered: Δg^{eff}([Fe^{IV}=O(TMP)]$^+$ > Δg^{eff}([Fe^{IV}=O(TDCPP)]$^+$) > Δg^{eff}([*Fe*^{IV}=O(TTMPP)]$^+$) (Figure 1). In the limit of strong coupling, the rhombic splittings of the spectra are attributed to the rhombicity of the total spin $S_t = {}^3/_2$, given by the expression $E_t/D_t = (2E - J_x^d + J_y^d)/(2D - 3J_z^d)$, which originates from the combined effects of local rhombicity E/D of the ferryl iron and of anisotropy in $\bar{J}$.[18] In the explicit spin-Hamiltonian analysis, it is possible to resolve the individual influences on the spectra. The resulting local rhombicity parameters, given in Table III, are ordered: E/D([Fe^{IV}=O(TMP)]$^+$) ≈ E/D([Fe^{IV}=O(TDCPP)]$^+$) > E/D([Fe^{IV}=O(TTMPP)]$^+$).

Resonance Raman Spectra. The resonance Raman spectra of the ferric starting complexes [Fe^{III}(Tf)TDCPP] and [Fe^{III}(Tf)TTMPP] in methylene chloride/methanol-d_4 in the high frequency range with 406.7-nm excitation (top trace; Figure 4a,b) are similar to the spectrum of [Fe^{III}(Tf)TMP] under the same conditions, shown for reference (top trace; Figure 4c). On oxidation to an oxoferryl porphyrin π cation radical by mCPBA, the resonance Raman spectrum of the TMP complex is characterized by downshifts of the marker bands[36,37] ν_2, ν_{11}, and ν_4 from 1652, 1492, and 1369 cm^{-1} to 1514, 1452, and 1327 cm^{-1}, respectively; this is identical to the published behavior[20] (middle trace; Figure 4c). Oxidation by mCPBA results in a similar pattern of behavior for the resonance Raman spectra of the TDCPP and TTMPP complexes (middle trace; Figure 4a,b). Addition of excess imidazole to the oxidized solutions regenerates spectra of ferric species[16,38] (bottom trace; Figure 4a–c). Thus the sequence of traces indicates that oxoferryl porphyrin π cation radicals [Fe^{IV}=O(TDCPP)]$^+$ and [Fe^{IV}=O(TTMPP)]$^+$ have been reversibly generated, in support of the spin-coupled ferryl porphyrin π radical electronic structure proposed for the oxidized intermediates.

Conclusion. We have cleanly generated two new high-valent iron porphyrin species in a methylene chloride/methanol-d_4 solvent mixture and have characterized the complexes by an array of spectroscopic techniques. We were able to establish the structures as oxoferryl porphyrin π cation radical species in which the ferryl and porphyrin π radical spins are parallel-coupled, as in the case of the TMP complex [Fe^{IV}=O(TMP)]$^+$. The high-frequency resonance Raman data obtained indicate that the porphyrin ligands of the new complexes studied are π cation radicals. A quantitative analysis of the EPR data of the three species indicates that the zero-field splitting parameters D and the isotropic iron(IV)-radical spin coupling constant J° are of similar magnitude in [Fe^{IV}=O(TMP)]$^+$ and [Fe^{IV}=O(TDCPP)]$^+$ and slightly smaller in [Fe^{IV}=O(TTMPP)]$^+$. Anisotropy contributions ($\bar{J}^d$) to spin coupling cannot be neglected when exchange and zero-field interactions are of the same order of magnitude, as is also observed in HRP-I[2] and CPO-I.[11] Relatively small components of $\bar{J}^d$ compared to J° (Table III) have significant influence on simulated EPR and Mössbauer spectra. Obviously, with $|J^\circ|/D \approx 1$, the wave functions of spin states are mixed to the extent that they become sensitive to small magneto-structural influences. We want to point out here that anisotropy contributions $\bar{J}^d$ are most likely due to admixtures of excited-state effects into the ground state, because dipolar contributions are estimated to be smaller by an order of magnitude than the values given in Table III. In summary, the Mössbauer data obtained for [Fe^{IV}=O(TMP)]$^+$ and [Fe^{IV}=O(TDCPP)]$^+$ are completely consistent with the data obtained by EPR spectroscopy for these compounds.

Acknowledgment. This work was supported by the Centre National de la Recherche Scientifique (UA 424), USPHS Grants ES03433 (A.G.) and GM34443 (J.T.) and the Deutsche Forschungsgemeinschaft. R.W. thanks the A. von Humboldt Foundation for financial support. A.G. and R.W. also thank NATO for a collaborative research grant.

(36) Abe, M.; Kitagawa, T.; Kyogoku, Y. *J. Chem. Phys.* **1978**, *69*, 4526–4534.
(37) (a) Czernuszewicz, R. S.; Macor, K. A.; Li, X. Y.; Kincaid, J. R.; Spiro, T. G. *J. Am. Chem. Soc.* **1989**, *111*, 3860–3869.
(38) Terner, J.; Sitter, A. J.; Reczek, C. M. *Biochim. Biophys. Acta* **1985**, *828*, 73–80.